



US 20240002310A1

(19) **United States**

(12) **Patent Application Publication**  
Wang et al.

(10) **Pub. No.: US 2024/0002310 A1**

(43) **Pub. Date:**  
**Jan. 4, 2024**

(54) **METHOD AND SYSTEM FOR UNZIPPING POLYMERS FOR ENHANCED ENERGY RELEASE**

(71) Applicants: **THE REGENTS OF THE UNIVERSITY OF CALIFORNIA**, Oakland, CA (US); **The Board of Trustees of the University of Illinois**, Urbana, IL (US)

(72) Inventors: **Haiyang Wang**, Riverside, CA (US); **Michael R. Zachariah**, Riverside, CA (US); **Jeffrey S. Moore**, Savoy, IL (US); **Mayank Garg**, Urbana, IL (US)

(73) Assignees: **THE REGENTS OF THE UNIVERSITY OF CALIFORNIA**, Oakland, CA (US); **The Board of Trustees of the University of Illinois**, Urbana, IL (US)

(21) Appl. No.: **18/343,137**

(22) Filed: **Jun. 28, 2023**

**Related U.S. Application Data**

(60) Provisional application No. 63/357,327, filed on Jun. 30, 2022.

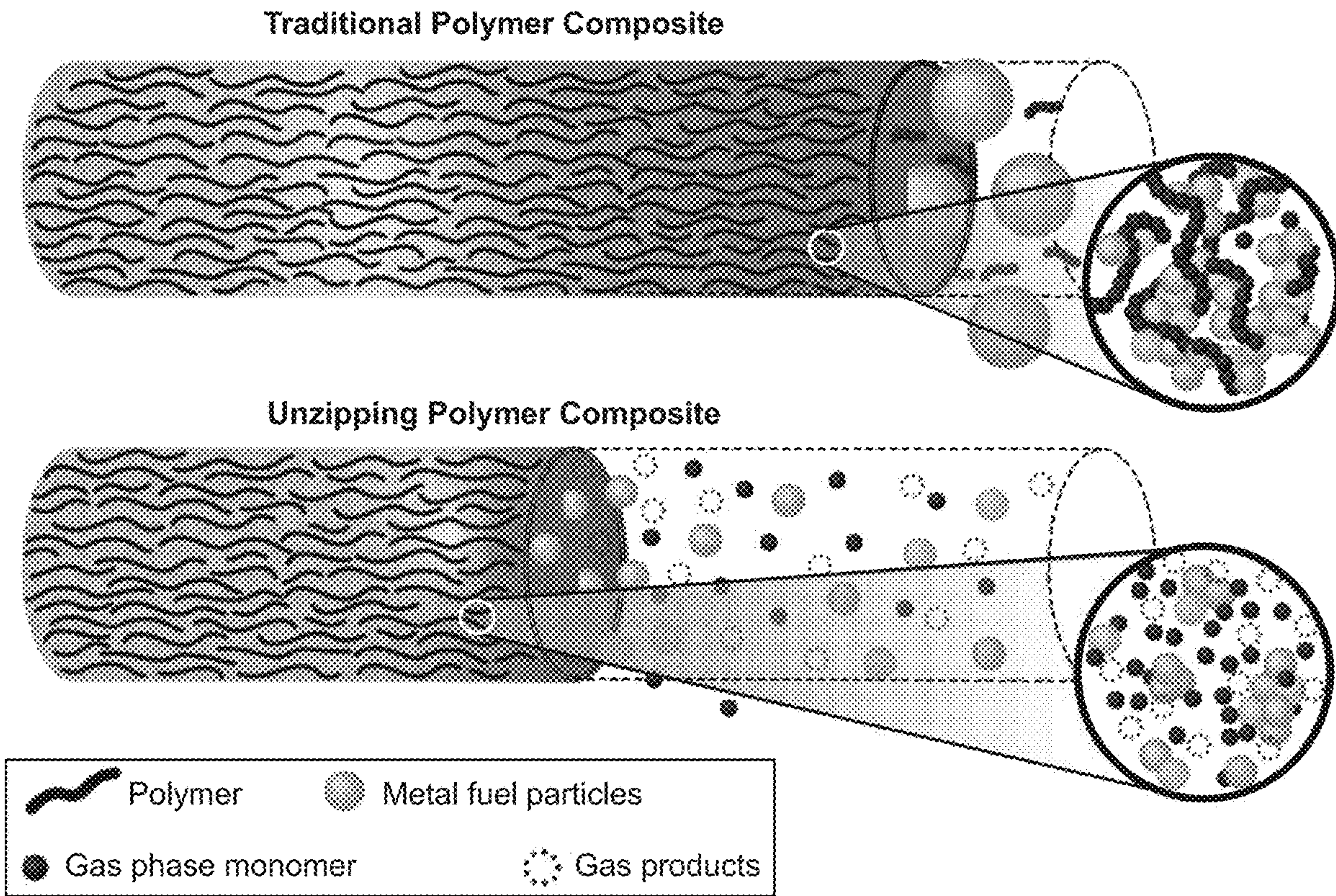
**Publication Classification**

(51) **Int. Cl.**  
**C06B 33/02** (2006.01)  
**C06B 47/02** (2006.01)  
**C06B 23/00** (2006.01)

(52) **U.S. Cl.**  
CPC ..... **C06B 33/02** (2013.01); **C06B 47/02** (2013.01); **C06B 23/00** (2013.01)

(57) **ABSTRACT**

An energetic composition and a method of unzipping polymer binders are disclosed, which includes localizing a heat feedback just near the reaction front by unzipping polymer binders employed to a nanothermite. The energetic composition includes an unzipping polymer binder employed to high load fuel and oxidizer particles.





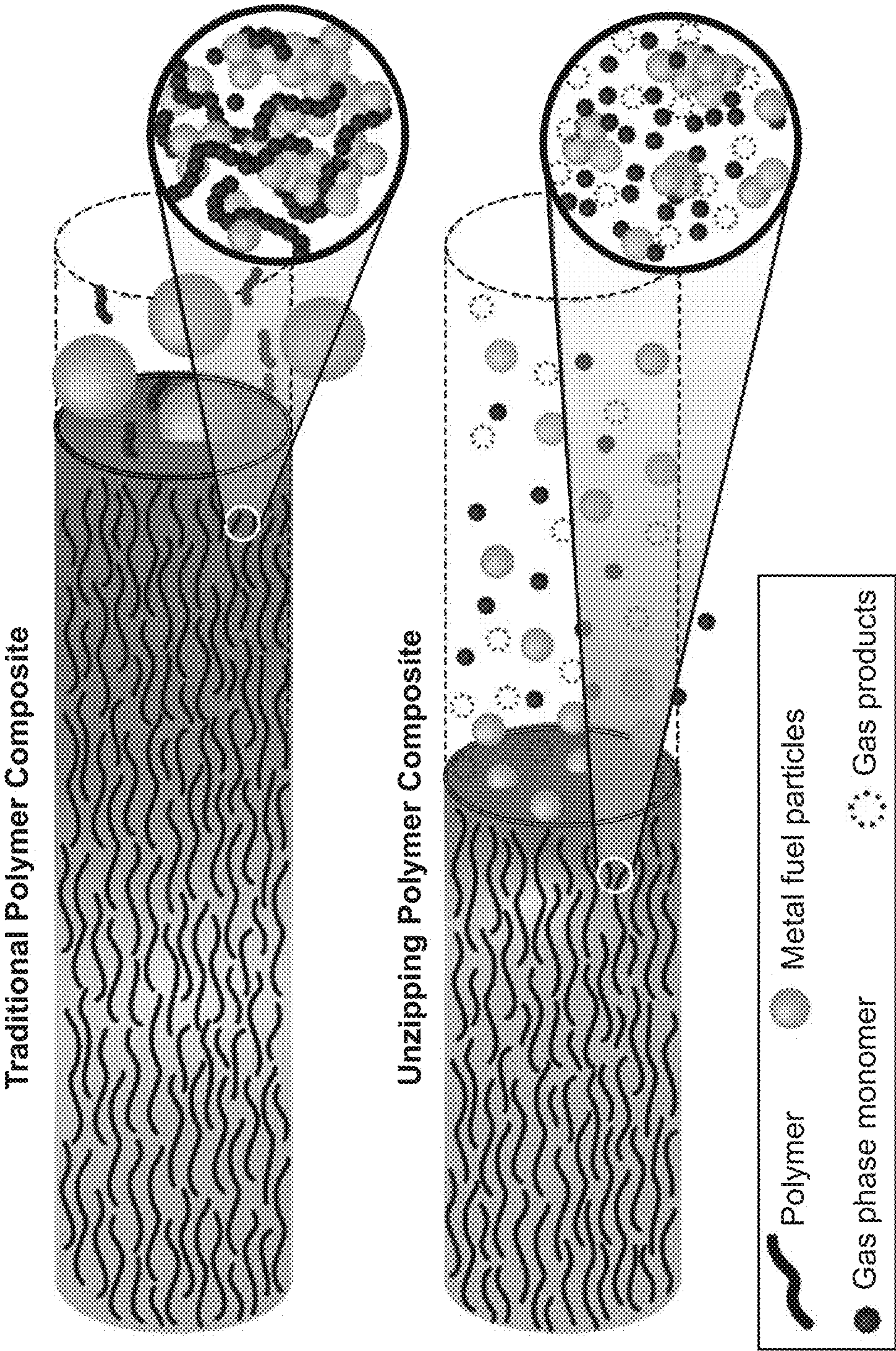


FIG. 1



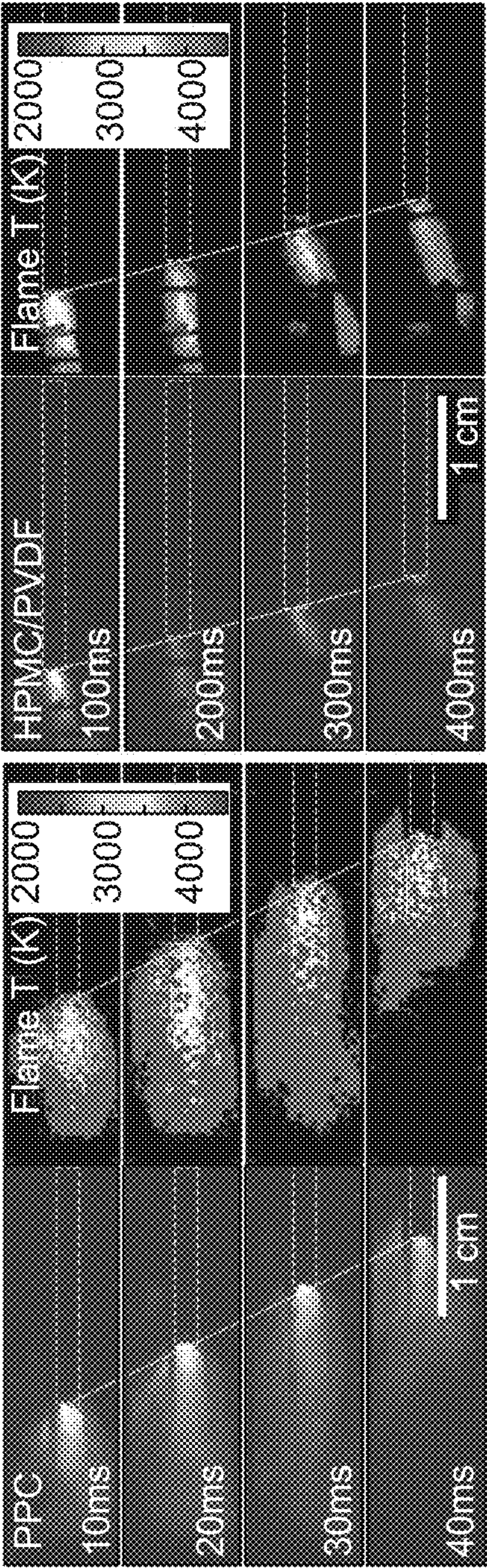


FIG. 2A

FIG. 2B

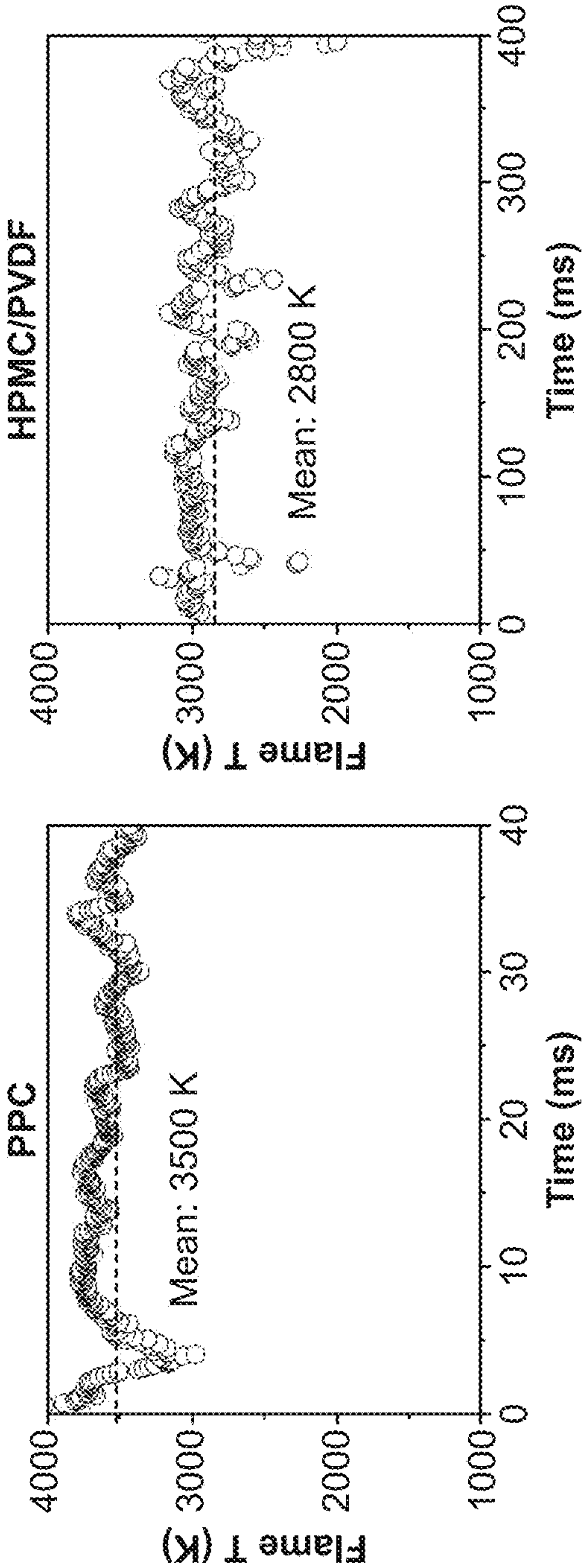


FIG. 2C

FIG. 2D



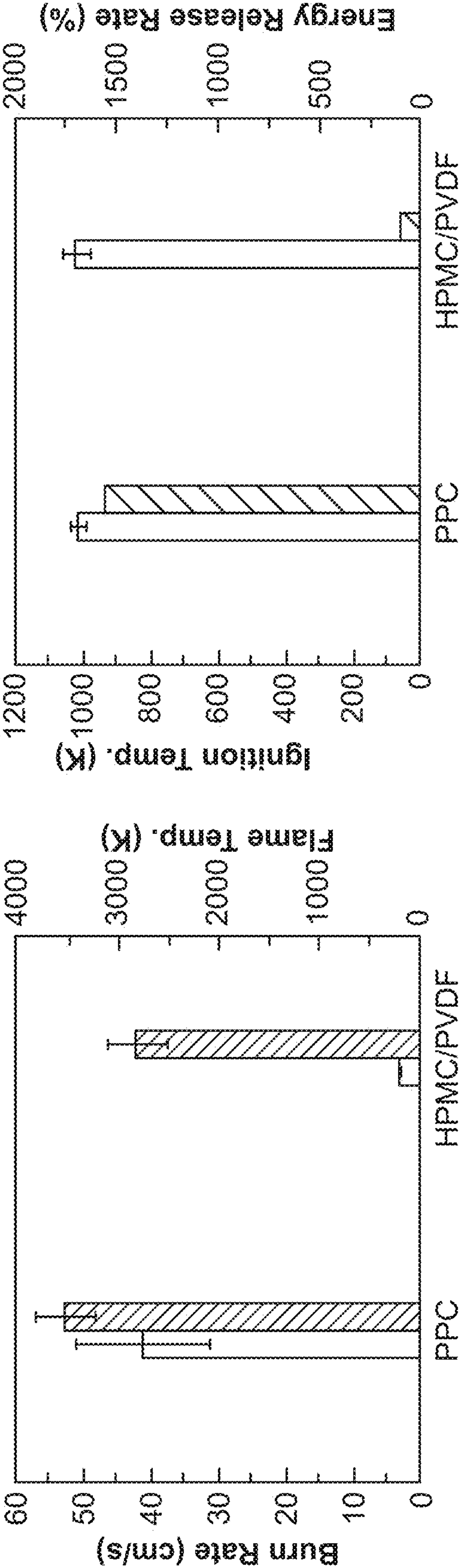


FIG. 3A

FIG. 3B



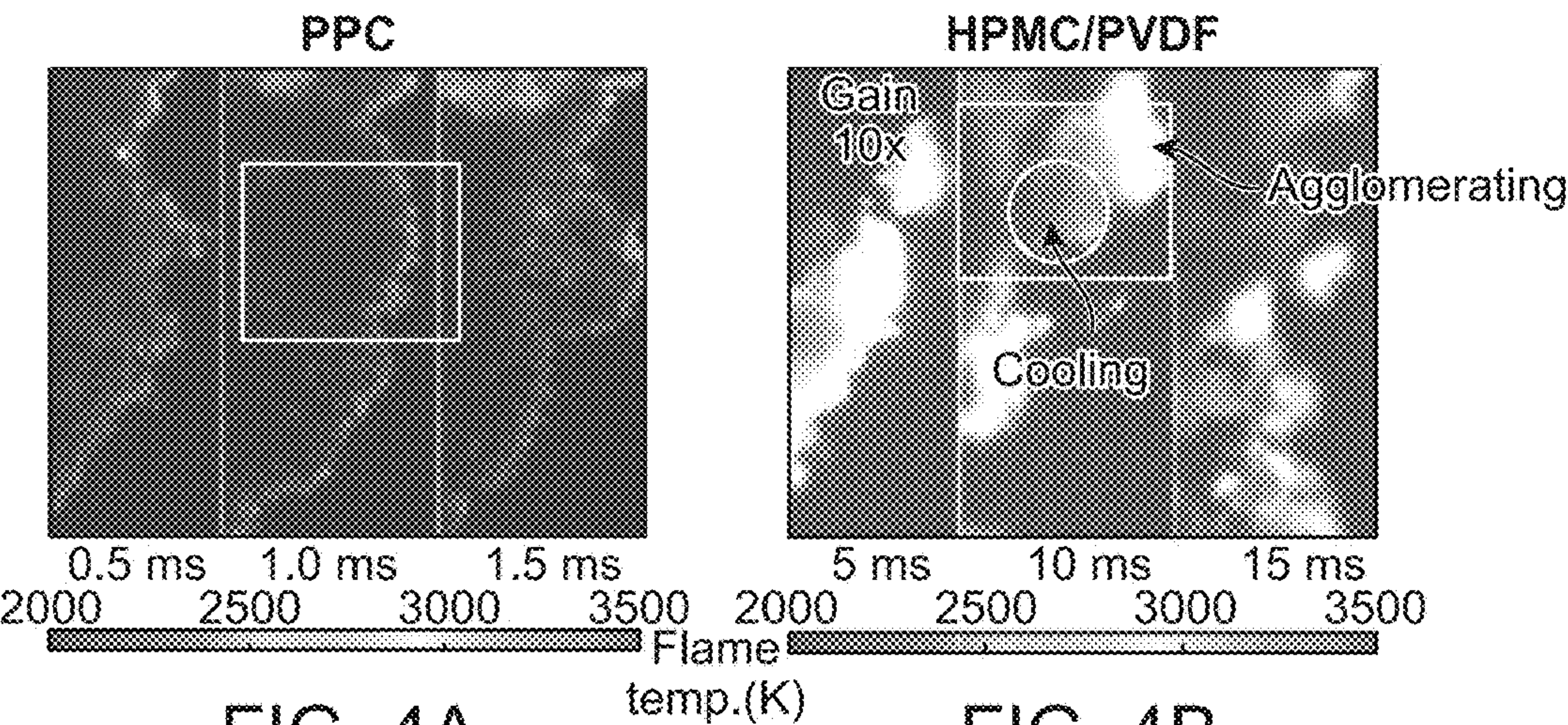


FIG. 4A

FIG. 4B

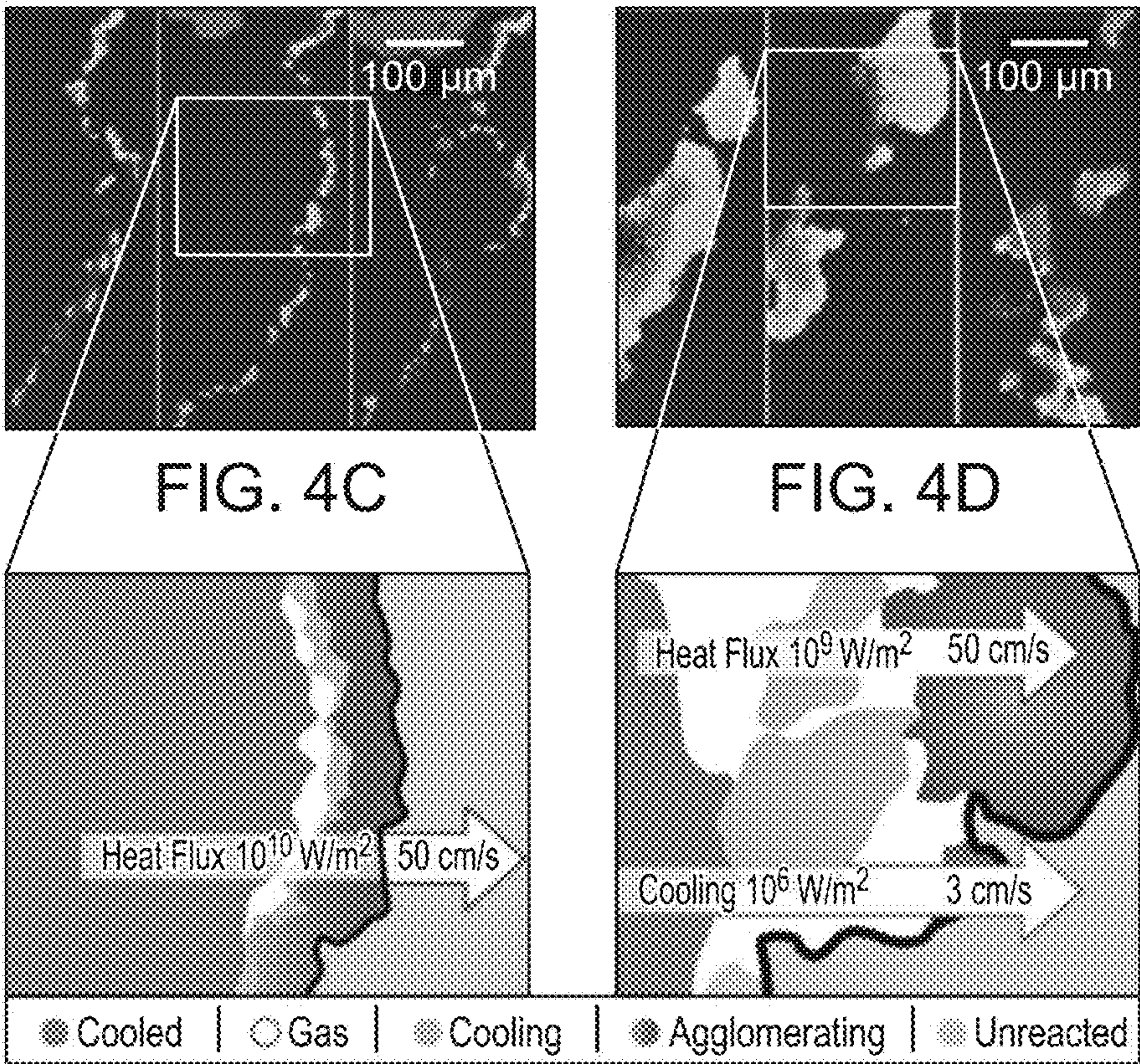


FIG. 4C

FIG. 4D

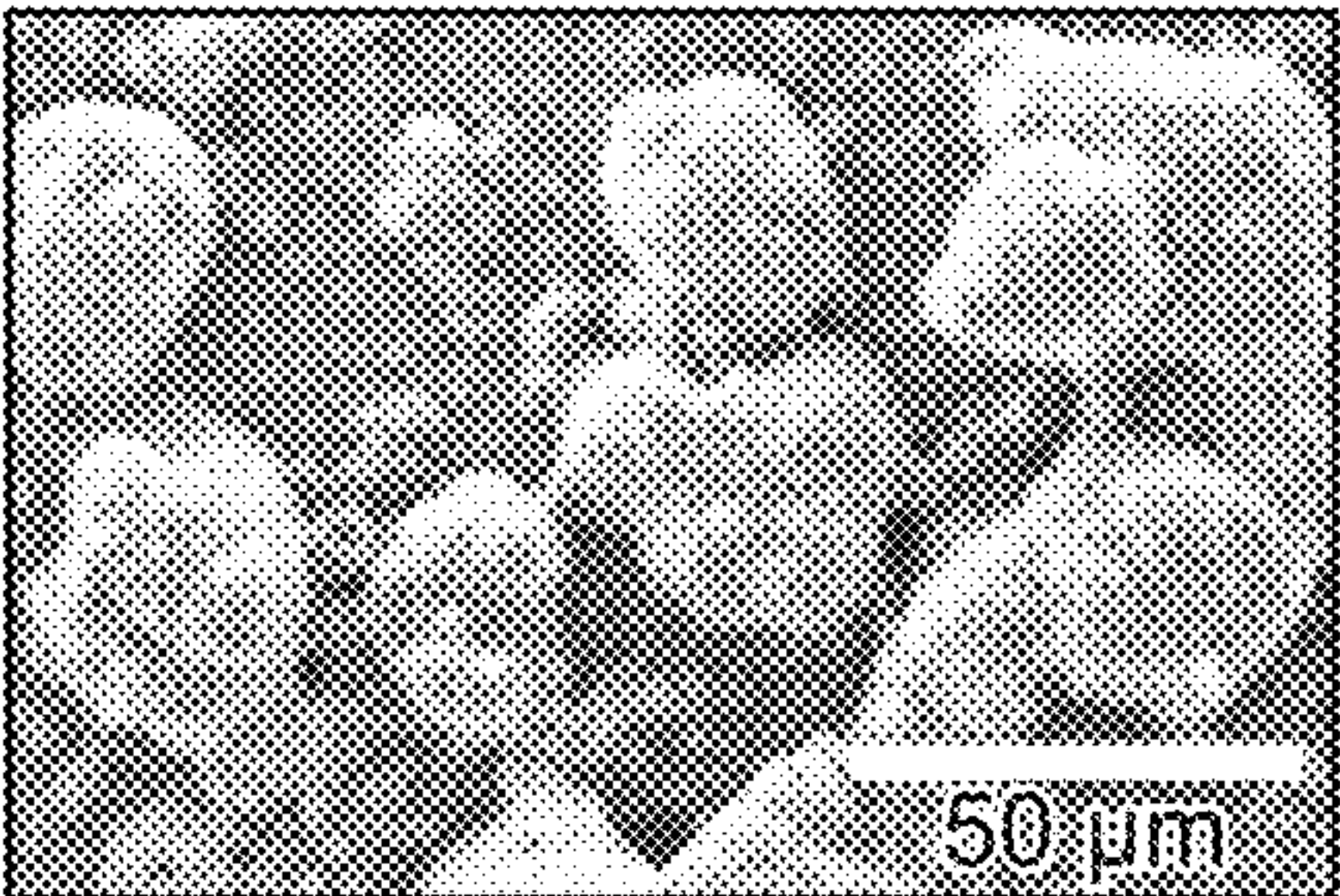
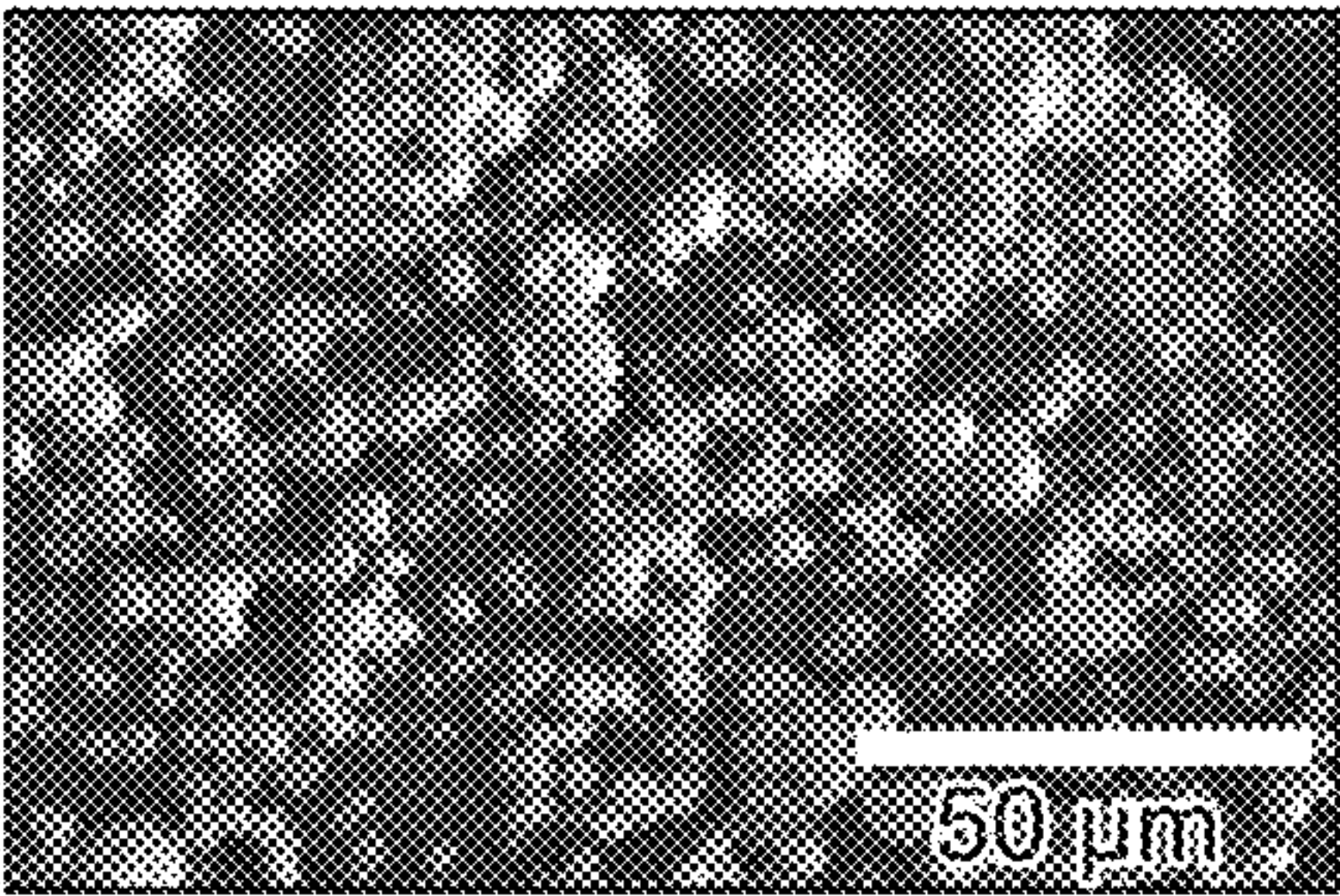


FIG. 4E

FIG. 4F

FIG. 4G

FIG. 4H



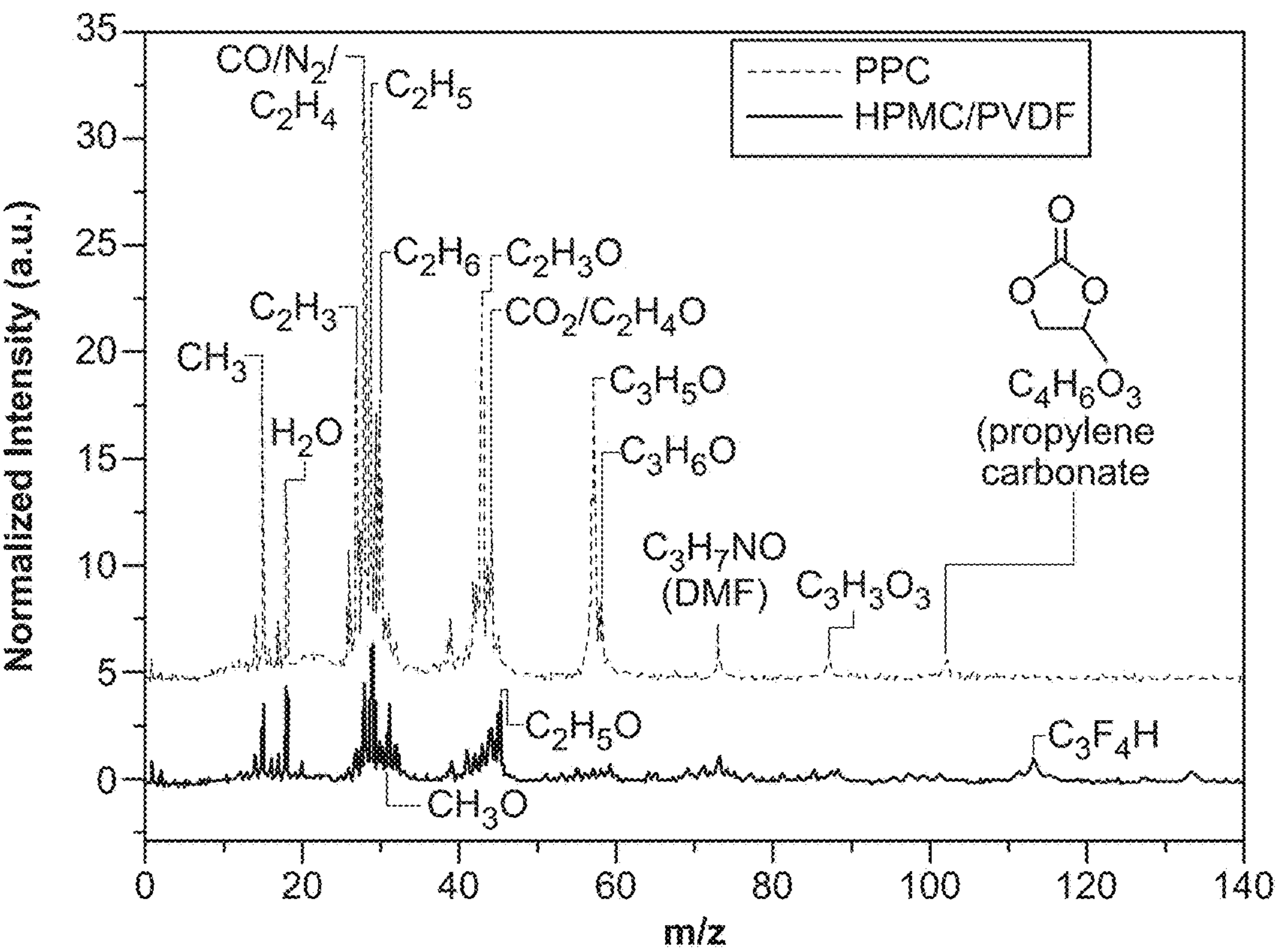


FIG. 5A

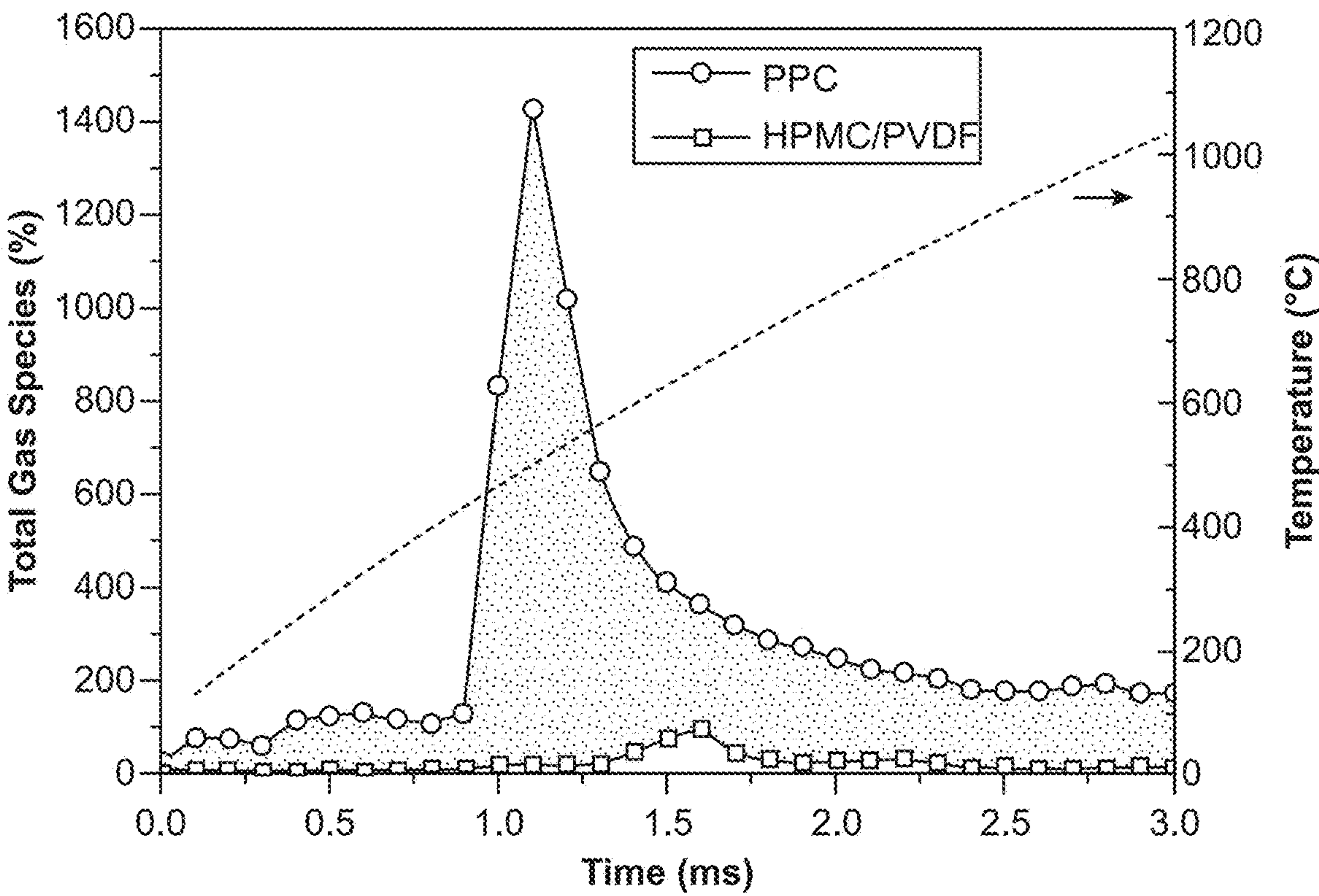


FIG. 5B



## METHOD AND SYSTEM FOR UNZIPPING POLYMERS FOR ENHANCED ENERGY RELEASE

### CROSS-REFERENCES TO RELATED APPLICATIONS

[0001] This application claims priority to U.S. Patent Application No. 63/357,327 filed on Jun. 30, 2022, the entire content of which is incorporated herein by reference.

### GOVERNMENT CLAUSE

[0002] This invention was made with government support under grant number N00014-21-1-2038 awarded by the Office of Naval Research. The government has certain rights in this invention.

### TECHNICAL FIELD

[0003] The present disclosure generally relates to a method and system for unzipping polymers for enhanced energy release, and more particularly, a method and system for unzipping polymer binders for enhanced energy flux of aluminized composites.

### BACKGROUND

[0004] Metal fuels such as aluminum (Al) have energy densities of  $\approx 30$  kJ/g ( $\approx 80$  kJ/cm<sup>3</sup>) with O<sub>2</sub>, which can be greater than 3 times ( $>3\times$ ) higher than the most powerful explosives such as hexanitrohexaazaisowurtzitane (CL-20). For this reason, Al particles are commonly employed as additives in various energetic materials such as propellants, explosives, and pyrotechnics. Nanoscale metallic fuels have been shown to be as much as 1000 times (1000 $\times$ ) more reactive than their micron-sized counterparts due to their high surface area to volume ratio. Unfortunately, significant sintering occurs on a time scale often shorter than the combustion time, which transforms the initial nanoscale fuel into microscale particles. This increase in particle size effectively slows down the energy release rate and mitigates some of the advantages of employing nanoscale metals.

[0005] To mitigate this problem, one strategy has been to preassemble the nanocomponents into larger microparticles, containing a gas-generator triggered to react at temperatures below the ignition temperature of the metallic fuel. The gas generator ejects and separates the individual nanoparticles (NPs) to reduce sintering and coalescence. While this approach has shown considerable promise, it requires subsequent processing to create free-standing structures by assembling the microparticles with additional polymer binders.

### SUMMARY

[0006] In accordance with an embodiment, a new approach is disclosed to enhance the energy delivery rate of energetic composites by employing an unzipping polymer. A greater than ( $>$ ) 1500% faster energy release rate of the aluminothermic reaction (Al/CuO) is disclosed, which has a thinner reaction front (e.g., 6 times) and a higher amount of gas species (e.g., 14 times) compared to the traditional polymer.

[0007] An energetic composition is disclosed, comprising: an unzipping polymer binder employed to high load fuel and oxidizer particles.

[0008] A method is disclosed of unzipping polymer binders comprising: localizing a heat feedback just near the reaction front by unzipping polymer binders employed to a nanothermite.

[0009] The energetic composition and the method of unzipping polymer binders can be employed, for example, in a propellant or a munition.

### BRIEF DESCRIPTION OF THE DRAWINGS

[0010] FIG. 1 is a conceptualization of unzipping vs traditional polymer binder, wherein the unzipping results in increased gas phase products near front that leads to less particle sintering, and further promotes a higher burn rate and a narrower reaction front with smaller agglomerations compared to traditional polymer composite.

[0011] FIGS. 2A-2D are illustrations of typical temporal burning snapshots, corresponding temperature maps (FIGS. 2A and 2B); time-resolved temperature profiles (FIGS. 2C and 2D) of 90 wt % Al/CuO particle loading composites with PPC (FIGS. 2A and 2C) and HPMC/PVDF (FIGS. 2B and 2D).

[0012] FIGS. 3A and 3B are illustrations of burn rate and flame temperature (FIG. 3A), ignition temperature and energy release rate (FIG. 3B) of 90 wt. % particle loading Al/CuO composites with PPC and HPMC/PVDF.

[0013] FIGS. 4A-4H are illustrations of microscopic snapshots (FIG. 4A and FIG. 4B), corresponding flame temperature map (FIG. 4C and FIG. 4D) and schematic showing (FIG. 4E and FIG. 4F) the flame fronts of 90 wt. % particle loading Al/CuO composites with PPC and HPMC/PVDF. SEM images and size distribution (FIG. 4G and FIG. 4H) of combustion products from Al/CuO with PPC (FIG. 4G) and HPMC/PVDF (FIG. 4H).

[0014] FIGS. 5A and 5B are illustrations of T-jump mass spectrum results of PPC and HPMC/PVDF (FIG. 5A); temporally integrated T-Jump mass spectra (FIG. 5B); temporal total gas release showing lower release temperature and significantly enhanced gas release for PPC case. Note: FIG. 5B is a sum of top-10 gas species in FIG. 5A.

### DETAILED DESCRIPTION

[0015] In accordance with an embodiment, an approach is disclosed to enhance the energy delivery rate of propellants and pyrotechnics by employing an unzipping polymer. The approach includes localizing the heat feedback to just near the reaction front by driving the endothermic chemistry of unzipping, which then liberates gas near the flame front and propel particles away from the burning surface, which minimizes agglomeration and sintering.

[0016] In this disclosure, the unzipping polymer can be a polycarbonate, for example, polypropylene carbonate (PPC), a poly(phthalaldehyde), for example, cyclic poly(phthalaldehyde) (cPPA), or a poly(vinyl ether sulfone), which can be employed to high load fuel and oxidizer particles to form an energetic composition. The high load fuel and oxidizer particles can include, for example, aluminized propellants, or nanothermites. In addition, polycarbonates such as disclosed in Fritz et al., Polycarbonates as temporary adhesives, *International Journal of Adhesion and Adhesives*, Vol. 38, October 2012, Pages 45-49, and Reed et al., Fabrication of microchannels using polycarbonates as sacrificial materials, *Journal of Micromechanics and Micro-engineering*, Volume 11, Number 6 (12 Oct. 2001), and



poly(vinyl ether sulfone)s such as disclosed in Lee et al., Tunable Thermal Degradation of Poly (vinyl butyl carbonate sulfone)s via Side-Chain Branching, *ACS Macro Letters*, Volume 4, Number 7 (21 Jul. 2015) can also be used as the unzipping polymer binder in the formation of the energetic composition.

**[0017]** In accordance with an embodiment, polypropylene carbonate (PPC) can be employed to load, for example, 90 wt % Al and CuO nanoparticles (NPs) via direct ink-writing. The results show a greater than 1500% (>1500%) faster energy release rate from the aluminothermic reaction compared to a conventional polymer binder. Through in-operando microscopy, a 6× thinner flame front and smaller combustion products were observed, revealing significantly lower agglomeration of Al NPs with the unzipping polymer. Fast-heating Time-of-Flight Mass Spectrometry confirms that the unzipping polymer decomposes to low molecular weight gases at a relatively low temperature, which significantly reduces the sintering of Al NPs. The thinner flame implies that heat feedback to the unreacted materials is more localized and drives the endothermic unzipping reaction for gas generation. A new approach is disclosed, which substantially increase the energy release rate of nanoscale metallic fuels.

**[0018]** A new approach is disclosed that utilizes a chain unzipping polymer (polypropylene carbonate, PPC) as a binder for energetic composite. PPC decomposes primarily through sequential monomer depolymerization. In accordance with an embodiment, the strategy is to localize the heat feedback to just near the reaction front by driving the endothermic chemistry of unzipping, which then liberates gas near the flame front and propel particles away from the burning surface, to minimize agglomeration and sintering. The basic concept is illustrated in FIG. 1.

**[0019]** In accordance with an embodiment, composites specimens were produced containing 90 wt % nanothermite and 10% wt % PPC binder using a direct-ink-writing process and demonstrate >15× energy release rate compared to a conventional polymer binder mixture (hydroxypropyl methylcellulose/polyvinylidene fluoride, HPMC/PVDF). High-speed microscopic imaging during combustion reveals a much thinner flame front (1/6×) and lower molecular weight combustion products with PPC, confirming our hypothesis of decreased sintering. Fast-heating Time-of-Flight Mass Spectrometry further confirmed that the unzipping polymer decomposes into volatiles at a relatively low temperature, which significantly reduces the sintering of Al NPs.

**[0020]** In accordance with an embodiment, Al/CuO was chosen as Al/CuO is a studied fuel/oxidizer combinations and PPC ( $M_w \approx 196$  kDa) was chosen as an unzipping, gas-generating polymer binder. The choice of PPC can be predicated that PPC has shown that depolymerization predominantly occurs through an unzipping mechanism to release propylene carbonate and carbon dioxide at temperatures near 250° C., and thus below the ignition threshold for the fuel. While other unzipping polymer are known, polymers that undergo chain unzipping depolymerization via radical intermediates (like polymethyl methacrylate, PMMA, and polystyrene, PS) tend to leave behind char, presumably because they crosslink. PPC is considered to depolymerize by chain unzipping mechanisms that do not involve radical intermediates resulting in better-behaved outcomes (no char, only forms monomer) when depolymerizing from condensed (neat) neat phases. The other thing to

note is that the temperature at which chain unzipping begins for PMMA and PS is considerably higher than PPC. The PPC can contain, for example, a 1 wt % photoacid generator (PAG) catalyst, which could be photolytically-activated with ultraviolet (UV) irradiation under standard ambient conditions or thermally activated at temperatures as low as  $\approx 180^\circ$  C., which could in principle be used to modulate the flame with contactless pre-processing approaches. For the control, a 90 wt % Al/CuO loading ink formulation based on a polymer hybrid (1:1 by mass) of Hydroxypropyl Methylcellulose (HPMC,  $M_w$  86 kDa) and Polyvinylidene fluoride (PVDF,  $M_w$  534 kDa) can be used. For example, HPMC gels upon heating via hydrophobic interactions and crosslinks with PVDF. In contrast, PPC is a thermoplastic that solidifies upon evaporation of the ink solvent dimethylformamide (DMF), which enables one to form free-standing composite sticks of 90 wt % Al and CuO NPs with only  $\approx 10$  wt % polymer.

**[0021]** To prepare an ink for printing, the binder can be dissolved in DMF, and a stoichiometric ratio of Al and CuO NPs are dispersed in the solution. The inks are directly written into a pre-designed square pattern on a heated glass substrate to facilitate solvent evaporation before writing a second layer. The printed sticks (15 layers) show smooth, crack-free surfaces, with a dense packing. The density of the composites is determined by combining the cross-sectional area, length, and mass of the specimens. The resulting value of  $\approx 1.6$  g/cm<sup>3</sup> approaches the theoretical packing density of NPs' aggregates (40%), further confirming the dense packing of NPs in these printed stick composites. SEM cross-sections of the printed sticks also reveal close packing of these NPs but microscale aggregates of the Al ( $\approx 80$  nm) and CuO ( $\approx 40$  nm) NPs are present. For example, all three Al/CuO composite sticks have similar morphology, density, and NPs dispersion.

**[0022]** Typical flame propagation snapshots (from left to right) of the composite sticks along with the flame temperature maps are shown in FIG. 2A (PPC) and FIG. 2B (HPMC/PVDF). All combustion tests were conducted in 1 atm argon to exclude additional oxygen from air. The flame fronts proceed steadily for both samples and demonstrate a stable linear burn rate. The first and most important difference is that Al/CuO with PPC propagates at  $\approx 40$  cm/s, which is  $\approx 13\times$  faster than with HPMC/PVDF ( $\approx 3$  cm/s). The flame temperature was obtained using a RGB color ratio based pyrometry technique and the detailed time-resolved profiles are shown in FIGS. 2C and 2D. The combustion of Al/CuO composite sticks with PPC (FIGS. 2A and 2C) show a much larger and hotter exhaust flame with an average flame temperature of  $\approx 3500$  K. The flame temperature is  $\approx 700$  K lower for the control sample shown in FIGS. 2B and 2D. The difference in flame temperatures indicates a large amount of hot gas/particle generation during PPC decomposition. The flame temperature of PPC-based composite ( $\approx 3500$  K) is higher than the adiabatic flame temperature of Al/CuO ( $\approx 2840$  K), for example, which is known for Al/CuO nanolaminates. This "super-adiabatic" discrete combustion arises, for example, in conditions where the chemistry is much faster than the heat dissipation.

**[0023]** A comparison of the combustion performance by measuring the burn rate, flame temperature, ignition temperature, and energy release rate of the different composites is summarized in FIGS. 3A and 3B. The composites with PPC burn at a speed of  $\approx 40$  cm/s, which is  $>13\times$  higher than



the HPMC/PVDF case (FIG. 3A). Assuming the cross-sectional area and the heat capacity of each composite is roughly the same, the burn rate, density, and flame temperature are combined to obtain the relative energy release rate. The composite with PPC binder shows a remarkable  $>15\times$  energy release rate compared to the HPMC/PVDF binder (FIG. 3B). In contrast, both composites have similar ignition temperatures of  $\approx 700^\circ\text{C}$ ., which is slightly higher than the melting point of Al ( $\approx 660^\circ\text{C}$ .), and on par with the ignition temperature measured for the neat Al/CuO powder, which implies that any heat and gas released from early decomposition of the polymers did not influence the ignition of Al/CuO chemically.

#### Thinner Flame Front and Reduced Agglomerations

**[0024]** As previously mentioned, upon melting, NPs agglomerate/sinter into greater than ( $>$ )  $1\text{ }\mu\text{m}$  scale particles during combustion, increasing the effect burning particle size by greater than  $20\times$  and significantly influencing the energy release rate. To assess if the unzipping impacted sintering, and the unzipping's relationship to a  $\approx 15\times$  increase in propagation, a microscopic imaging was employed with a spatial and temporal resolution of  $\sim\mu\text{m}$  and  $\sim\mu\text{s}$ . Typical snapshots with temperature maps of the flame fronts are shown in FIGS. 4A-4H, for the Al/CuO with PPC and HPMC/PVDF, respectively. The flame front for PPC composite is much thinner, and more continuous compared to HPMC/PVDF composite. Specifically, the thickness of the flame front for PPC is only  $\approx 5\text{ }\mu\text{m}$ - $10\text{ }\mu\text{m}$ , which is about 10% of the thickness of the control. FIGS. 4A-4H collectively suggests that the flame front consists of agglomerations of NPs with sizes that are similar to the thickness of the flame front. With HPMC/PVDF and schematically shown in FIG. 4F, the discontinuous flame front suggests inhomogeneous reaction with heat fluxes during sintering ( $10^9\text{ W/m}^2$ ) and cooling ( $10^6\text{ W/m}^2$ ), supporting two different local (microscopic) propagating speeds of  $\approx 50\text{ cm/s}$  and  $\approx 3\text{ cm/s}$ , respectively. The overall macroscopic burn rate ( $\approx 3\text{ cm/s}$ ) is limited by the slow step of cooling. By contrast, the flame front with PPC (FIG. 4E) is continuous, consisting of smaller particles with a  $\approx 10\times$  higher heat flux of  $\approx 10^{10}\text{ W/m}^2$ , which significantly enhances macroscopic flame propagating velocity to  $\approx 50\text{ cm/s}$  (more details are in supporting videos). Consistent with the flame temperatures shown in FIG. 3A, the flame front of the PPC case shows higher temperatures (more yellow/red, less blue) compared to that of HPMC/PVDF. The post-combustion product SEM images (FIGS. 4G and 4H) and size distribution confirm much smaller sintered particles for the PPC composite ( $\approx 4\text{ }\mu\text{m}$ ) compared to the HPMC/PVDF case (mean:  $\approx 32\text{ }\mu\text{m}$ ). The microscopic high-speed videos and corresponding time-resolved temperature maps of the free-standing composite sticks further confirm that significantly smaller particles are produced and ejected from the burning surfaces from PPC compared to HPMC/PVDF.

#### Unzipping Polymer Promotes Higher Gas Generation

**[0025]** In accordance with an embodiment, the unzipping polymer acts as an efficient gas generator. PPC and HPMC/

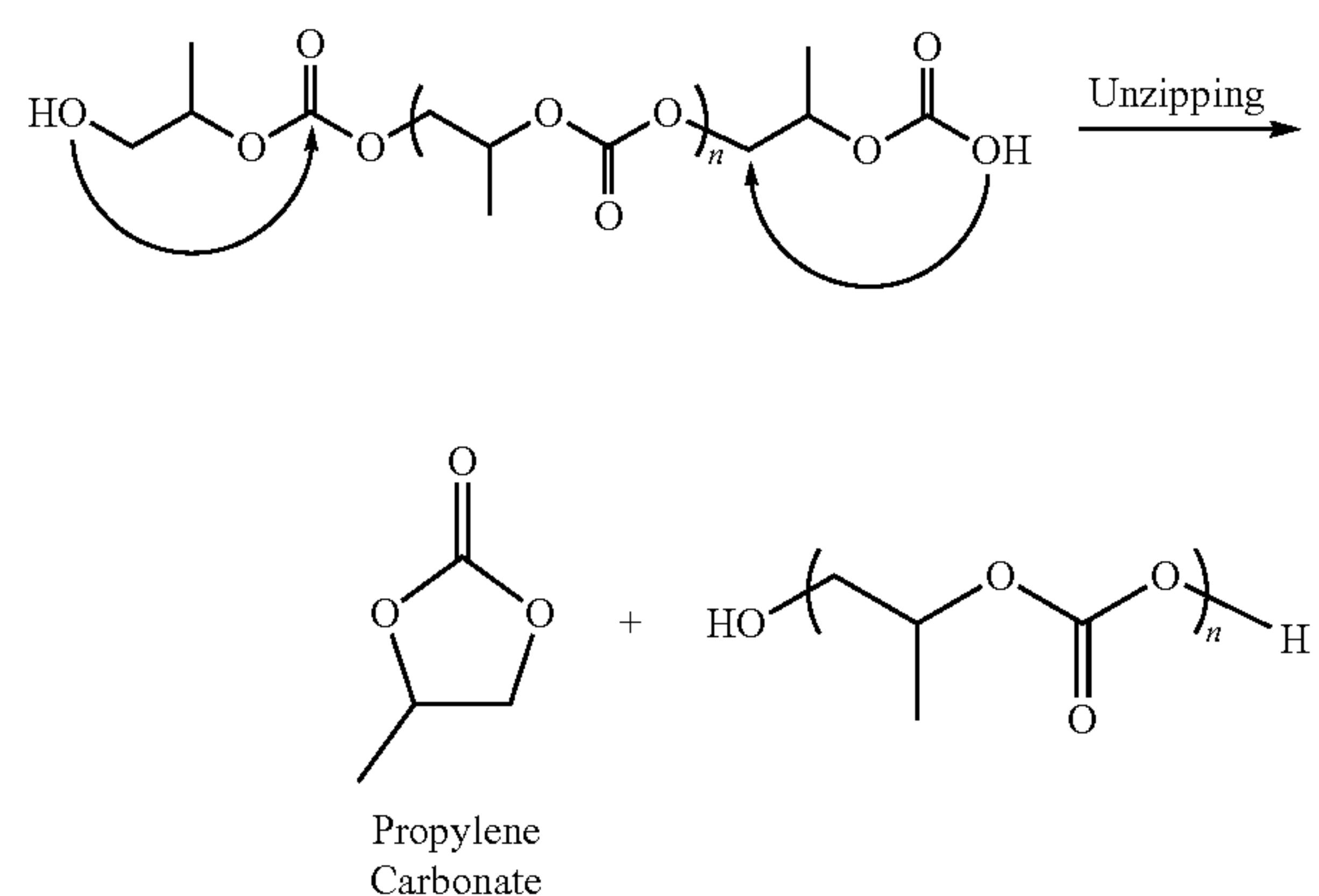
PVDF were coated on a thin ( $70\text{ }\mu\text{m}$ ) joule heated platinum wire to study decomposition at a heating rate of  $\approx 4\times 10^5\text{ K}\cdot\text{s}^{-1}$ . The T-jump wire is coupled to a time-of-flight mass spectrometer capable of acquiring complete spectra at  $10,000\text{ Hz}$ . FIG. 5A shows mass spectra for the two cases and clearly indicate that PPC releases a significantly high amount of gas phase species. Integrating the spectral peaks enables one to quantify the relative amount of gas and is presented as a sum total of gas produced as a function of molecular mass. FIG. 5B shows a  $14\times$  increase in gas production for PPC compared to HPMC/PVDF.

**[0026]** Since PVDF contains no oxygen and leaves a significant amount of solid carbon residue upon decomposition. In contrast, PPC depolymerizes into gaseous monomers ( $m/z=102$ ,  $\text{C}_4\text{H}_6\text{O}_3$ ) at a temperature as low as  $350^\circ\text{C}$ . These gaseous monomers ( $\approx 350^\circ\text{C}$ .) further decompose into lighter species and peaks at  $\approx 500^\circ\text{C}$ . (FIG. 5B), i.e., below the Al melting point ( $660^\circ\text{C}$ .). This low temperature gas decomposition should eject the NPs from the burning surface and minimize agglomerating/sintering (schematically shown in FIG. 1). On the other hand, half of the gas generation from HPMC/PVDF is  $m/z>60$  (FIG. 5A) and maximizes at a higher temperature at  $\approx 650^\circ\text{C}$ . (FIG. 5B) and very near the Al melting point where sintering is expected to be severe.

**[0027]** The thermal decomposition of PPC primarily occurs via two mechanisms: (i) polymer unzipping (Equation 1), and (ii) random chain scission (Equation 2). In accordance with an embodiment, it is notable that there is a weak peak for  $\text{CO}_2$  ( $m/z=44$ ) release at an earlier temperature of  $\approx 300^\circ\text{C}$ ., which is attributed to random chain scission of PPC (Equation 2). The most prominent species detected are propylene carbonate ( $m/z=102$ ) and its fragments, indicating that unzipping (Equation 1) is the primary pathway.

(1)

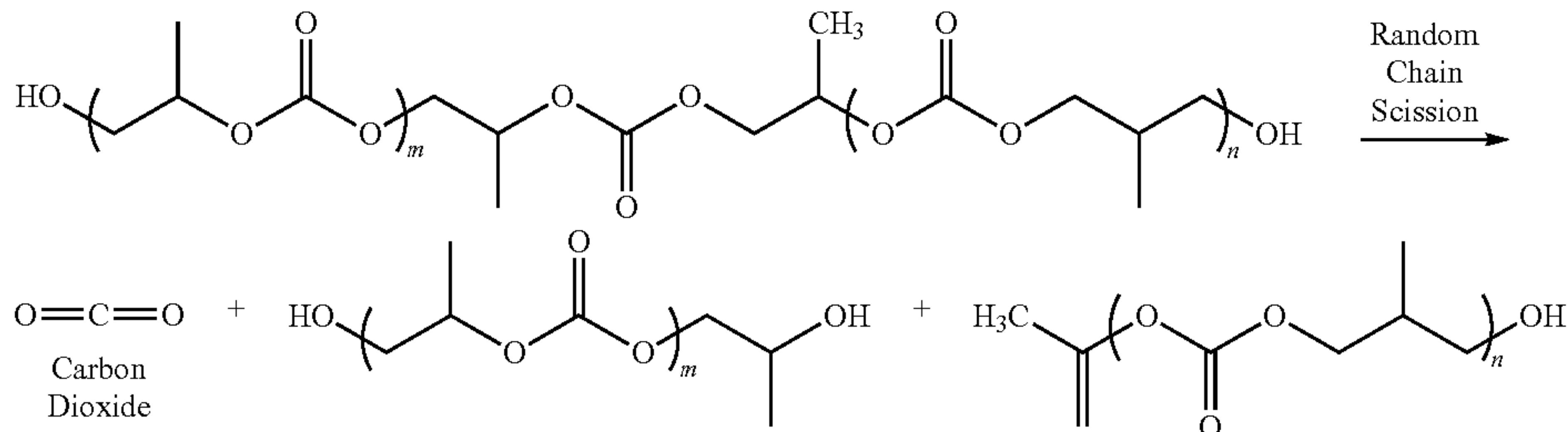
Equation 1





Equation 2

(2)



**[0028]** In accordance with an embodiment, the integrated mass spectra show gas release 14× higher, this corresponds remarkable close to the ≈15× increase in burn rate and further evidence that unzipping is directly related to the enhanced energy release rate.

**[0029]** In accordance with an embodiment, using a polymer binder (PPC) that undergoes sequential unzipping to generate low molecular weight fragments, results in propagation velocities of a nanoparticle fuel/oxidizer composite that are significantly enhanced. For the example of Al/CuO composites, energy delivery rates of 15 times higher than our previously developed hybrid polymer thermite composites. The flame temperature of PPC-based Al/CuO is also ≈700 K higher than that of the HPMC/PVDF case. The burning of PPC-based Al/CuO composites has a flame front consisting of small agglomerations with a thickness ≈5 μm-10 μm, which is ≈10% of that previously observed for HPMC/PVDF case. T-Jump mass spectrometry show that upon fast heating PPC depolymerizes to deliver a greater than (>) 14X increase in small molecular weight gaseous products which significantly reduces NP agglomeration/sintering and dramatically enhances flame propagation and energy release rate. The results of the work are thus consistent with the original hypothesis as presented in FIG. 1. The results point to developing polymer systems that employ unzipping to more efficiently utilize heat feedback to locally drive endothermic depolymerization, with large monomer production leading to reduced sintering of the metallic fuel and presumably a more complete combustion.

#### Experimental Section

**[0030]** Chemicals: Hydroxypropyl Methylcellulose (HPMC, brand name: METHOCEL™ F4M) has a molecular weight ( $M_w$ ) of 86 kDa and a viscosity of 4,000 cP (2% solution, 25° C.). Polyvinylidene fluoride (PVDF,  $M_w$  534 kDa) and N, N-Dimethylformamide (DMF, 99.8%) were purchased from Sigma-Aldrich. Poly(propylene carbonate) (PPC) pellets ( $M_w$  ≈196 kDa) were gifted by Novomer. 4-Methylphenyl [4-(1-methylethyl) phenyl] iodonium tetakis (pentafluorophenyl) borate photoacid generator (PAG) catalyst, commercially known as Rhodorsil-FABA, was supplied by Bluestar Silicones. CuO nanoparticles (≈40 nm) were purchased from US Research Nanomaterials. Aluminum nanoparticles (Al NPs, ≈50 nm) have an active content is ≈67 wt. % according to thermogravimetric/differential scanning calorimetry (TG/DSC) results.

**[0031]** Ink Preparation: To prepare a stable ink for direct writing, 100 mg HPMC/PVDF (1:1 by mass) or PPC (with

or without 1% PAG) was separately weighed and dissolved in 3.2 mL DMF and magnetically stirred for ≈2 hrs to get a clear solution. Then 668.6 mg CuO and 231.4 mg Al NPs were dispersed into the above polymer solution by ultrasonication for ≈1 hr. Then the resulting slurry was magnetically and mechanically stirred for 24 hrs and 1 hr, respectively.

**[0032]** T-Jump Ignition and Mass Spectrum: The above-mentioned polymer inks with and without Al/CuO nanothermite were characterized by a T-Jump ignition and mass spectrum system, respectively. Ignition of Al/CuO composites and decomposition of polymers were conducted in argon and vacuum, respectively, to get the ignition temperatures and decomposition species. Typically, the inks were coated and dried on a ≈10 mm long platinum filament (≈76 μm in diameter), which was resistively heated to ≈1400 K at a heating rate of ≈4×10<sup>5</sup> K·s<sup>-1</sup> (in 1 atm argon or in vacuum). The temporal filament resistance (correlated via the Callendar-Van Dusen Equation) during the heating process was recorded. The ignition and subsequent combustion of the composites was monitored using a high-speed camera (Phantom V12.1) and the ignition temperatures are obtained by coupling the observed ignition timestamp from the high-speed video with the filament temperature.

**[0033]** Direct-ink-Writing Process: The obtained inks were extruded through an 18-gauge needle (inner diameter: 0.038" (≈0.96 mm)) at a feed rate of ≈9 mL/h and a printing speed (moving speed of the nozzle) of 25 cm/min. The substrate was kept at ≈75° C. to ensure removal of DMF and dry off the printing layer before depositing another layer. After printing, the samples were left on the heated substrate (kept at ≈75° C.) for another 30 mins to further evaporate any remaining solvent. The free-standing composite sticks were printed 15 layers with a square of 8 cm×8 cm and were cut into 3 cm long sticks for combustion characterization. The density and porosity are determined from the mass divided by the volume (cross-sectional area×length) of each stick. The porosity of the samples was estimated by (1-(actual density/theoretical density)). Al/CuO composites were also printed on the glass slides with 3 layers, for microscopic imaging of the flame front.

**[0034]** Morphology Characterization: The microstructure of the printed samples was investigated by using a ThermoFisher Scientific NNS450 scanning electron microscope (SEM) coupled with energy dispersive X-ray spectroscopy (EDS).

**[0035]** Macroscopic and microscopic imaging: All the combustion tests were conducted in argon (1 atm). The samples can be either free-standing burn sticks (≈1.5 cm



long, for both macroscopic and microscopic imaging) or composites on the glass slide ( $\approx 2.2$  cm long, for microscopic imaging only). The sticks or glass slides can be attached on a steel support using a double-side tape, and the support is mounted to a 3D translational stage for focus purpose. The macroscopic imaging high-speed camera (Vision Research Phantom Miro M110) has a resolution of  $\approx 80 \mu\text{m}/\text{pixel}$  while the microscopic imaging system (Vision Research Phantom VEO710L coupled to Infinity Photo-Optical Model K2 DistaMax) has a resolution of  $\approx 2 \mu\text{m}/\text{pixel}$ .

**[0036]** Burn Rate and Flame Temperatures: The linear burn rate ( $v$ ) and average flame temperature ( $T_{\text{flame}}$ ) of the composite sticks were determined from the macroscopic videos. The samples were ignited by nichrome wire. Before reaching steady state,  $<1$  mm of sample is consumed. The linear burn rate was calculated by dividing the length of the sample by the total burning time. The energy release rate considers densities ( $\rho$ ), burn rates ( $v$ ) and flame temperatures (energy release rate  $\sim \rho \times v \times T$ ) and is normalized to the control sample (HPMC/PVDF case) assuming all the three composites have the same specific heat capacity and cross-sectional area. Briefly, three channel intensity (red, green, blue) ratios are extracted from a color camera. These data are processed using a house-built MATLAB routine and demosaiced for the camera's Bayer filter using standard MATLAB algorithms. The system was calibrated with a black-body source (Mikron, Oriel) and the corresponding flame temperature maps were output and reported. The estimated temperature uncertainty is  $\approx 200$  K-300 K.

**[0037]** Supporting macroscopic and microscopic combustion videos of the free-standing Al/CuO composite sticks with 10 wt % HPMC/PVDF, 10 wt % neat PPC and 10 wt % PPC (1% PAG), respectively. Supporting microscopic combustion videos through the back of glass slides: Al/CuO composites with 10 wt % HPMC/PVDF and 10 wt % as received PPC, respectively. Low and higher magnification cross-sectional SEM images of the printed composite sticks, SEM/EDS (Scanning electron microscopy (SEM) and energy dispersive X-ray spectroscopy (EDS)) and size distributions of the combustion products, burn rates, flame temperatures and energy release rate of all the printed samples: Al/CuO composite sticks with 10 wt % HPMC/PVDF, 10 wt % PPC (1% PAG), and 10 wt % neat PPC.

**[0038]** The detailed description above describes embodiments of a method and system for unzipping polymers for enhanced energy release. The invention is not limited, however, to the precise embodiments and variations described. Various changes, modifications and equivalents may occur to one skilled in the art without departing from the spirit and scope of the invention as defined in the accompanying claims. It is expressly intended that all such changes, modifications and equivalents which fall within the scope of the claims are embraced by the claims.

What is claimed is:

1. An energetic composition, comprising:  
an unzipping polymer binder employed to high load fuel and oxidizer particles.
2. The energetic composition of claim 1, wherein the unzipping polymer is a polycarbonate, a poly(phthalaldehyde), a poly(vinyl ether sulfone), or a combination of unzipping polymers.
3. The energetic composition of claim 1, wherein the unzipping polymer is polypropylene carbonate (PPC) or cyclic poly(phthalaldehyde) (cPPA).
4. The energetic composition of claim 3, wherein the fuel and oxidizer particles are Al and CuO nanoparticles (NPs).
5. The energetic composition of claim 4, wherein the unzipping polymer is 10 wt % PPC or cPPA, and the high load fuel and oxidizer particles is 90 wt % Al and CuO nanoparticles (NPs).
6. The energetic composition of claim 5, wherein the 10 wt % PPC or cPPA is loaded with the 90 wt % Al and CuO nanoparticles (NPs) by direct ink-writing, and wherein the PPC or cPPA decomposes through sequential monomer depolymerization.
7. The energetic composition of claim 1, wherein the unzipping polymer binding employed to the high load fuel and oxidizer particles is employed in a propellant or a munition.
8. The energetic composition of claim 1, wherein the high load fuel and oxidizer particles are nanothermites.
9. The energetic composition of claim 1, wherein the high load fuel and oxidizer particles include aluminized composites.
10. A method of unzipping polymer binders comprising:  
localizing a heat feedback just near the reaction front by unzipping polymer binders employed to a nanothermite.
11. The method of claim 10, wherein the unzipping polymer is a polycarbonate, a poly(phthalaldehyde), a poly(vinyl ether sulfone), or a combination of unzipping polymers.
12. The method of claim 10, wherein the unzipping polymer is polypropylene carbonate (PPC) or cyclic poly(phthalaldehyde) (cPPA).
13. The method of claim 12, further comprising:  
decomposing the polypropylene carbonate (PPC) or the cyclic poly(phthalaldehyde) (cPPA) through sequential monomer depolymerization.
14. The method of claim 12, further comprising:  
loading the polypropylene carbonate (PPC) or the cyclic poly(phthalaldehyde) (cPPA) with the nanothermite by direct ink-writing to form an energetic composition.
15. The method of claim 14, wherein nanothermite comprises Al and CuO nanoparticles (NPs).
16. The method of claim 14, further comprising:  
employing the energetic composite in a propellant or a munition.
17. The method of claim 10, wherein the nanothermite includes Al and CuO nanoparticles (NPs).

\* \* \* \* \*